

## Oxygen vacancies induced switchable and nonswitchable photovoltaic effects in Ag/Bi<sub>0.9</sub>La<sub>0.1</sub>FeO<sub>3</sub>/La<sub>0.7</sub>Sr<sub>0.3</sub>MnO<sub>3</sub> sandwiched capacitors

R. L. Gao, H. W. Yang, Y. S. Chen, J. R. Sun, Y. G. Zhao, and B. G. Shen

Citation: [Applied Physics Letters](#) **104**, 031906 (2014); doi: 10.1063/1.4862793

View online: <http://dx.doi.org/10.1063/1.4862793>

View Table of Contents: <http://scitation.aip.org/content/aip/journal/apl/104/3?ver=pdfcov>

Published by the [AIP Publishing](#)

---

### Articles you may be interested in

[Switchable photovoltaic response from polarization modulated interfaces in BiFeO<sub>3</sub> thin films](#)

Appl. Phys. Lett. **104**, 142903 (2014); 10.1063/1.4870972

[Photovoltaic effect of lead-free \(Na<sub>0.82</sub>K<sub>0.18</sub>\)<sub>0.5</sub>Bi<sub>4.5</sub>Ti<sub>4</sub>O<sub>15</sub> ferroelectric thin film using Pt and indium tin oxide top electrodes](#)

J. Appl. Phys. **115**, 034107 (2014); 10.1063/1.4862401

[The effect of polarization fatigue process and light illumination on the transport behavior of Bi<sub>0.9</sub>La<sub>0.1</sub>FeO<sub>3</sub> sandwiched capacitor](#)

J. Appl. Phys. **113**, 183510 (2013); 10.1063/1.4804308

[Influence of work-function of top electrodes on the photovoltaic characteristics of Pb<sub>0.95</sub>La<sub>0.05</sub>Zr<sub>0.54</sub>Ti<sub>0.46</sub>O<sub>3</sub> thin film capacitors](#)

Appl. Phys. Lett. **100**, 173901 (2012); 10.1063/1.4705425

[Photovoltaic characteristics in polycrystalline and epitaxial \(Pb<sub>0.97</sub>La<sub>0.03</sub>\)\(Zr<sub>0.52</sub>Ti<sub>0.48</sub>\)O<sub>3</sub> ferroelectric thin films sandwiched between different top and bottom electrodes](#)

J. Appl. Phys. **105**, 061624 (2009); 10.1063/1.3073822

---

An advertisement for KeySight B2980A Series Picoammeters/Electrometers. The ad features a red and white color scheme. On the left, text reads 'Confidently measure down to 0.01 fA and up to 10 PΩ' and 'KeySight B2980A Series Picoammeters/Electrometers'. Below this is a red button with the text 'View video demo >'. On the right, there is an image of the device and the KeySight Technologies logo.

## Oxygen vacancies induced switchable and nonswitchable photovoltaic effects in Ag/Bi<sub>0.9</sub>La<sub>0.1</sub>FeO<sub>3</sub>/La<sub>0.7</sub>Sr<sub>0.3</sub>MnO<sub>3</sub> sandwiched capacitors

R. L. Gao,<sup>1,2,a)</sup> H. W. Yang,<sup>2</sup> Y. S. Chen,<sup>2</sup> J. R. Sun,<sup>2,a)</sup> Y. G. Zhao,<sup>3</sup> and B. G. Shen<sup>2</sup>

<sup>1</sup>School of metallurgy and materials engineering, Chongqing University of Science and Technology, Chongqing 401331, China

<sup>2</sup>Beijing National Laboratory for Condensed Matter Physics and Institute of Physics, Chinese Academy of Science, Beijing 100190, China

<sup>3</sup>Department of Physics and State Key Laboratory of Low-Dimensional Quantum Physics, Tsinghua University, Beijing 100084, China

(Received 22 October 2013; accepted 7 January 2014; published online 22 January 2014)

The short circuit photocurrent ( $I_{sc}$ ) was found to be strongly dependent on the oxygen vacancies ( $V_{Os}$ ) distribution in Ag/Bi<sub>0.9</sub>La<sub>0.1</sub>FeO<sub>3</sub>/La<sub>0.7</sub>Sr<sub>0.3</sub>MnO<sub>3</sub> heterostructures. In order to manipulate the  $V_{Os}$  accumulated at either the Ag/Bi<sub>0.9</sub>La<sub>0.1</sub>FeO<sub>3</sub> or the Bi<sub>0.9</sub>La<sub>0.1</sub>FeO<sub>3</sub>/La<sub>0.7</sub>Sr<sub>0.3</sub>MnO<sub>3</sub> interface by pulse voltages, switchable or nonswitchable photocurrent can be observed without or with changing the polarization direction. The sign of photocurrent could be independent of the direction of polarization when the variation of diffusion current and the modulation of the Schottky barrier at the Ag/Bi<sub>0.9</sub>La<sub>0.1</sub>FeO<sub>3</sub> interface induced by oxygen vacancies are large enough to offset those induced by polarization. Our work provides deep insights into the nature of photovoltaic effects in ferroelectric films, and will facilitate the advanced design of switchable devices combining spintronic, electronic, and optical functionalities. © 2014 AIP Publishing LLC. [<http://dx.doi.org/10.1063/1.4862793>]

Multiferroics, which combine ferroelectric and magnetic orders, and the possibility of coupling between magnetic and ferroelectric order parameters, thus enabling manipulation of one through the other, have attracted a considerable number of attentions in recent years because of their potential applications in multifunctional novel devices, such as the spintronics, multistate data storage, magnetic filter, and various sensors.<sup>1,2</sup> Among them, single-phase multiferroic BiFeO<sub>3</sub> (BFO) is one of the most studied lead-free multiferroic materials due to its high ferroelectric ( $T_C = 1103$  K) and antiferromagnetic ( $T_N = 643$  K) transition temperatures and large ferroelectric polarization of  $100 \mu\text{C}/\text{cm}^2$  in thin films.<sup>3,4</sup> Recently, the photovoltaic (PV) effect observed in BFO has received increasing interest due to its small band gap ( $\sim 2.8$  eV) and switchable diode and PV effects.<sup>5–10</sup> It was found that the orientation of photocurrent and diode-like rectifying characteristics were strongly depended on the polarization switching, the direction of the diode and PV effects can be reversibly switched by applying an alternating electric field, and the sign of photocurrent related to the diode effect is always opposite to the polarization direction.<sup>7,8</sup> Thus, it is believed that polarization flipping should play an essential role in the observed diode switching and PV effects.<sup>5,7,8</sup> However, several sensitive experiments show that the migration of positively charged oxygen vacancies ( $V_{Os}$ ) under an external electric field is as essential as the polarization flipping in producing the switchable diode and PV effects,<sup>5</sup> and even the critical parameter for defining such phenomenon in BFO based thin films.<sup>11</sup> It also indicated that the sign of

photocurrent is independent of the direction of polarization, but it is always opposite to the voltage direction of the last treatment.<sup>11</sup> Obviously, whether the oxygen vacancies or the polarization or both of them affect the PV effects is quite elusive. Besides the oxygen vacancies and polarization, the formation of a Schottky barrier at the metal–semiconductor interface is also reported to have a contribution to the PV effect.<sup>12–14</sup> Therefore, it would be of great value to disentangle how oxygen vacancies, polarization, and Schottky barriers interact with each other to affect the PV effects of ferroelectric films.

Herein, we report the influences of  $V_{Os}$  on the photovoltaic effects in Ag/Bi<sub>0.9</sub>La<sub>0.1</sub>FeO<sub>3</sub>/La<sub>0.7</sub>Sr<sub>0.3</sub>MnO<sub>3</sub> sandwiched capacitors. According to manipulate the distribution of  $V_{Os}$  by pulse voltages, we observed switchable photocurrent without changing the polarization direction; moreover, the sign of photocurrent could be the same although the polarization direction was switched. The variation of diffusion current and the modulation of the Schottky barrier at the Ag/Bi<sub>0.9</sub>La<sub>0.1</sub>FeO<sub>3</sub> interface induced by oxygen vacancies are believed to responsible for this result.

Using pulsed laser deposition (PLD), Bi<sub>0.9</sub>La<sub>0.1</sub>FeO<sub>3</sub> (BLFO) thin films with the thickness of 500 nm were epitaxially grown on (001) oriented SrTiO<sub>3</sub> (STO) single crystal substrates with 30 nm La<sub>0.7</sub>Sr<sub>0.3</sub>MnO<sub>3</sub> (LSMO) films as the buffer layers (used as a bottom electrode). The conductive metallic oxide LSMO was chosen because of their small lattice parameter mismatches and stress among LSMO, BLFO, and STO.<sup>14,15</sup> First LSMO thin films were deposited on STO substrates under a deposition temperature of 700 °C, and an oxygen pressure ( $P_{O_2}$ ) of 50 Pa. Then, the BLFO thin films were grown at 650 °C and 15 Pa.<sup>14,16</sup> Following the growth, these samples were then cooled to room temperature at 5 °C/min in 100 Pa  $P_{O_2}$ . For the conductive characteristics

<sup>a)</sup>Authors to whom correspondence should be addressed. Electronic addresses: gaorongli2008@163.com, Tel.: +86-23 -65023479, Fax: +86-23 -65023479 and jr.sun@iphy.ac.cn, Tel.: +86-10 -82648085, Fax: +86-10 -82649485.

measurements, 200 nm thick Ag layer as the top electrodes was deposited using PLD through a shadow mask with an area of  $3 \times 10^{-4} \text{ cm}^2$ . The crystal structure and surface of the samples were studied using X-ray diffraction (XRD) and atomic force microscopy (AFM), ferroelectric domains of the BFO films were studied using piezoelectric force microscopy (PFM). The  $P$ - $E$  hysteresis loops measurement was carried out using an AixACCT ferroelectric test unit at 10 kHz for BLFO samples. Current-voltage characteristics were measured using a Keithley 2611 source meter. Green laser with the wavelength of 532 nm ( $100 \text{ mW/cm}^2$ ) was used as excitation light source for the PV measurement.

Figure 1(a) shows the XRD patterns of our samples, which reveals high quality, epitaxial films that appear to be single phase. The (002) diffraction peaks of BLFO film are slightly higher than the  $45.770^\circ$  expected for pure BFO crystal [inset of Fig. 1(a)], suggesting that our BLFO films are weakly strained. We have also investigated the ferroelectric properties of these BLFO films using a combination of AFM, PFM, and polarization-electric field ( $P$ - $E$ ) hysteresis loop measurements. AFM imaging [Fig. 1(b)] of BLFO films reveals smooth films—average root mean square roughness (RMS) of 5.5 nm. PFM was used to probe the ferroelectric nature of the films. The films were poled through PFM tip scanning of the film surface by +10 V with a square area

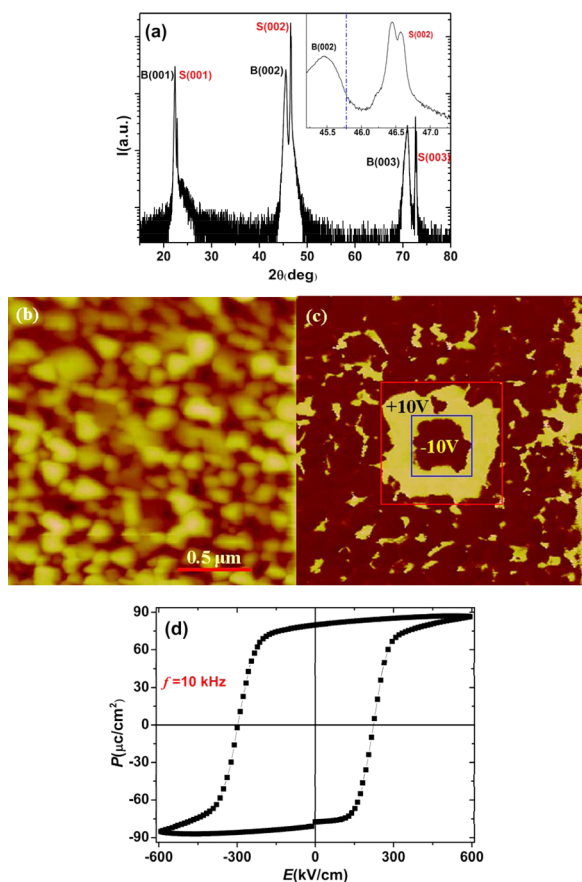


FIG. 1. (a) XRD spectrum of BLFO/LSMO/STO films, where the 002 peaks are amplified in insets and the dashed lines located at  $45.770^\circ$  expected for bulk like BFO. (b) Typical AFM image of BLFO/LSMO/STO (001) films with a square area  $2 \times 2 \mu\text{m}^2$ , indicating smooth surface and sphere-like grains. (c) Out of plane PFM images demonstrating switching of films. (d).  $P$ - $E$  loops of BLFO/LSMO/STO (001) thin films at  $f = 10 \text{ kHz}$ .

$1 \times 1 \mu\text{m}^2$ . After that, the polarization in the center  $0.5 \times 0.5 \mu\text{m}^2$  area is scanned by  $-10 \text{ V}$  voltage. Finally, the piezoelectric phase image was carried out by applying an ac voltage (frequency 6 kHz, amplitude 3 V peak-to-peak) to the PFM tip with a square area  $2 \times 2 \mu\text{m}^2$ . By applying a voltage to the tip during the scan, we were able to reversibly switch the polarization, as shown in [Fig. 1(c)]. Figure 1(d) shows the  $P$ - $E$  hysteresis loop measurements, revealing high quality, square-like hysteresis loops with a saturation polarization of  $\sim 80 \mu\text{C/cm}^2$ , which is slightly bigger than that of pure BFO films.<sup>4,17-20</sup>

The presence of a significant diode-like rectification effect but without switching of the rectification direction was observed in BLFO thin films [see Figure 2(a)]. For upward poling,  $-30 \text{ V}$  ( $\sim 600 \text{ kV cm}^{-1}$ ,  $20 \mu\text{s}$  duration) pulse was applied to the top Ag electrode of BLFO at room temperature (RT). In this paper, applying a positive (negative) voltage on the top electrode or tip is defined as downward (upward) poling. As shown in Figure 2(a), a rectification behavior with the bottom-to-top as the backward bias direction was observed after upward poling, however, the rectification direction can't be switched at all with downward poling by applying  $+30 \text{ V}$  pulses. The resistance state can be switched from low resistance state (LRS) to high resistance state (HRS) in the negative bias while the polarization direction switching from upward polarization state (UPS) to downward polarization state (DPS). These results demonstrate that the barrier height of BLFO/LSMO interface is always higher than that of Ag/BLFO interface both in UPS and DPS.<sup>16</sup>

To measure the intrinsic PV effect of BLFO, we illuminated on the top Ag electrode using a visible green light laser. Unwanted light illumination on the top electrodes and surfaces was avoided by covering with black tape. Repeatable switching of the PV current direction accompanying polarization switching and a good retention of the PV effect are demonstrated in Figure 2(b). Short-circuit current ( $I_{sc}$ ) direction is always opposite to the polarization direction and can be switched with polarization flipping but independent of the rectification directions, the  $I_{sc}$  after downward poling was  $-5.8 \text{ nA}$ , whereas the  $I_{sc}$  after upward poling was about  $+7.5 \text{ nA}$ . The  $I_{sc}$  measured as a function of time, exhibit little temporal change of photocurrent. In addition, we found no hint of photocurrent degradation when the  $I_{sc}$  was measured during 3 on-and-off cycles of the illumination light. Such good retention and high stability over multiple cycles are vital parameters for possible device applications.

The nonswitchable  $I_{sc}$  unveils the prominent role of oxygen vacancies ( $V_{O_s}$ ) in the PV effect of BLFO. First, BLFO was downward poled with  $-30 \text{ V}$  pulse at RT, similar to the situation in Figure 2(b). Subsequently, upward poling was achieved with  $-50 \text{ V}$  pulse for  $20 \mu\text{s}$  at 50 K, and then the  $I_{sc}$ - $t$  characteristic was measured at RT with the light is on and off for 3 cycles. On the contrary, BLFO was upward poled at RT, then downward poling was achieved with  $+50 \text{ V}$  pulses for  $20 \mu\text{s}$  at 50 K, and finally the  $I_{sc}$ - $t$  characteristic was measured at RT with the light is on and off for 3 cycles. The upward and downward poling and subsequent  $I_{sc}$ - $t$  measurement results are summarized in Figure 2(c). It can be observed from Fig. 2(c) that after upward poled at

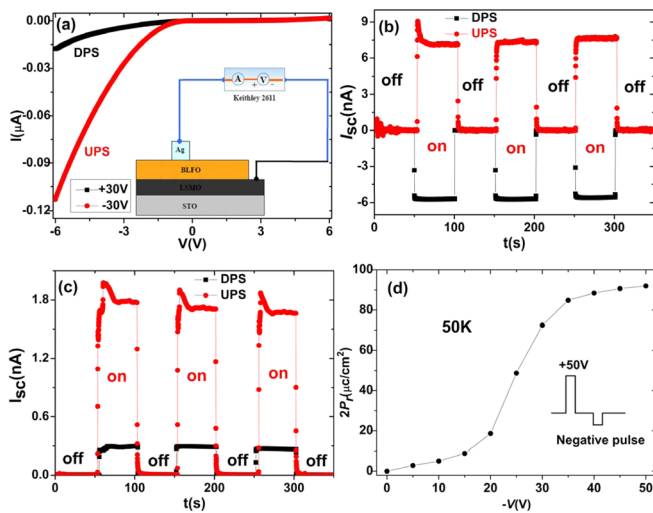


FIG. 2. (a)  $I$ - $V$  curves for the BLFO/LSMO/STO (001) films poled by +30 V (DPS) and -30 V (UPS) pulse voltages. Inset shows the schematic of  $I$ - $V$  measure circuit. (b) Time-dependent of short circuit photocurrent ( $I_{sc}$ ) for the DPS and UPS with light on and off. (c) Time-dependent of  $I_{sc}$  for the DPS with light on and off after applying -30 V at RT and then +50 V at 50 K and for the UPS with light on and off after applying +30 V at RT and then  $\pm 50$  V at 50 K (d) Voltage dependent of polarization (P-V curves) at 50 K.

50 K, the  $I_{sc}$  decrease to 1.8 nA, while it is 0.3 nA after downward poled at 50 K, which indicates that the orientation of  $I_{sc}$  cannot be switched with the polarization flipping at all. We should emphasize that the applied voltage ( $\pm 50$  V) is much larger than the ferroelectric coercivity ( $\sim 25$  V) and can fully poled the BLFO to DPS or UPS at 50 K [shown in Fig. 2(d)]. Therefore, our results imply that the polarization flipping is not sufficient to induce the full switching of the  $I_{sc}$  direction, and high-temperature (RT) flipping seems necessary to induce a good switching of the  $I_{sc}$  [see Fig. 2(b)].

In order to confirm the above implication that the switchable and nonswitchable  $I_{sc}$  is induced by  $V_{Os}$ , we have directly measured the time dependent of  $I_{sc}$  after applying consistent pulse voltages to the BLFO films so as to manipulate the  $V_{Os}$  accumulating at either the Ag/BLFO or the BLFO/LSMO interface. The  $I_{sc}$ - $t$  curves measurements with varying polarization direction and  $V_{Os}$  distribution were performed at RT and the results are shown in Figure 3. After applying -30 V pulses for different times to BLFO in the negatively poled state, the  $I_{sc}$ - $t$  curve was measured at 300 K. Polarization flipping has not occur because all the pulses are negative, but significant change of the  $I_{sc}$ - $t$  characteristic was observed, as shown in Fig. 3(a).  $I_{sc}$  is always positive and it increases with the number of negative pulses increasing, from the initial  $\sim 7.5$  nA to 13 nA after 1000 pulses. In contrast, after consistent negative pulses, a positive pulse of +30 V was applied to pole the BLFO films to be DPS. It can be seen from Fig. 3(b) that with increasing the number of negative pulses (-30 V), the  $I_{sc}$  gradually decreases, and the sign has been changed eventually with 1000 pulses. However, it can be observed from both Figs. 3(a) and 3(b) that the variation trend of  $I_{sc}$  (i.e.,  $\Delta I_{sc}$ ) is the same and  $I_{sc}$  is positive when applying consistent negative pulse voltages, independent of the polarization directions. Comparing Fig. 3(a) with 3(b), that the orientation of  $I_{sc}$  can be switched without changing the polarization direction; in

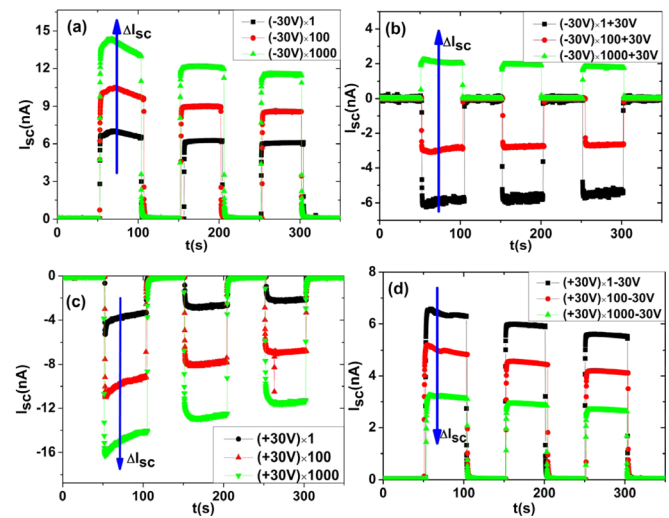


FIG. 3. Time-dependent of  $I_{sc}$  with light is on and off. (a) After applying successive negative pulse voltage (-30 V) strings (UPS). (b) After applying different successive negative pulse voltage (-30 V) strings and then applying different successive positive pulse voltage (+30 V) strings (DPS). (c) After applying successive positive pulse voltage (+30 V) strings (DPS). (d) After applying different successive positive pulse voltage (+30 V) strings and finally applying -30 V (UPS) on the samples. The arrows indicate the variation direction of  $I_{sc}$ .

other words, the sign of  $I_{sc}$  can be the same despite switching the polarization direction. Thus, we have confirmed that the ferroelectric polarization flipping alone is not sufficient to switch the  $I_{sc}$  direction, and consistent negative pulse voltage “forming” is an important ingredient for the switching. In addition, we have performed in-situ poling with consistent positive pulse voltages and subsequent measurements of  $I_{sc}$ - $t$  curves. It can be seen from Figs. 3(c) and 3(d) that  $\Delta I_{sc}$  is the same and  $I_{sc}$  is always negative both in UPS and DPS. Obviously, negative pulse voltages induce increasing and positive  $\Delta I_{sc}$  while positive pulse voltages produce the opposite results. The results shown demonstrate that the electromigration of defects, such as oxygen vacancies, is an important ingredient for the switchable and nonswitchable  $I_{sc}$ . As we will discuss below, consistent pulse voltage induces electromigration of oxygen vacancies, which influences electronic properties in a significant manner. Numerous scenarios have been suggested as the origin of the PV effect in BFO including asymmetric impurity potentials associated with depolarization field and polarization-dependent band bending at metal-ferroelectric interfaces.<sup>21–23</sup> Our results clearly demonstrate that the diode backward direction is independent of the PV current direction and polarization direction, suggesting that the scenario with a simple asymmetric impurity potential may not be dominant.

In order to fully understand the characteristics of switchable and nonswitchable PV effects in the BLFO samples mentioned above, schematic energy band diagrams should be established for the samples. Because oxygen vacancies are always present in perovskite oxides, it is reasonable to regard BLFO based thin films as an n-type semiconductor.<sup>15,24</sup> Considering the different work functions of Ag, BFO, LSMO, the electron affinity/band gap of BFO,<sup>25</sup> and the effects of ferroelectric polarization and oxygen vacancy layer on the interfacial barrier, the modulation of the energy band induced by the migration of oxygen vacancies and

polarization flipping can be sketched as shown in Figure 4, which can satisfactorily explain the direction of the photocurrent.

In general, the photocurrent has two contributions: diffusion current ( $I_{diffusion}$ ) and drift current ( $I_{drift}$ ).  $I_{diffusion}$  is related to the gradient of photo-induced electron-hole pair density. Electrons always diffuse from high density areas to low density regions, which form the so called diffusion current. While  $I_{drift}$  is affected by the internal electric field of the depletion layer, electrons moves as a result of the drift force of the electric field. On the one hand, the photo generated electron-hole pairs can drift toward/against the surface under the field  $E_{A-B}$  and  $E_{L-B}$  (Here,  $E_{A-B}$  and  $E_{L-B}$  indicates the electric field between Ag-BLFO and BLFO-LSMO, respectively). Considering the penetration depth of the illumination and that electrons are generated effectively near the top surface due to the illumination on top Ag electrode,  $I_{diffusion}$  and  $I_{drift}$  can be sketched as shown in Figure 4.

For the UPS case, a large  $I_{diffusion}$  flows to the downward direction (from Ag to LSMO in BLFO films) because photo-generated electrons diffuse effectively to the top electrode due to short traveling distance and thus a low probability of electro-hole recombination. Furthermore, the oxygen vacancies in the oxygen deficient film can trap the photo induced electrons and the photo induced holes become the extra carriers.<sup>26-29</sup> More  $V_{OS}$  accumulated at the Ag/BLFO interfaces means more photo induced holes move forward to LSMO bottom electrode. A tiny  $I_{drift}$  flows to the upward direction due to the small barrier height between Ag/BLFO interfaces. Therefore, a positive net photocurrent  $I_{sc}$  flows downward, as shown in Fig. 4(a). In the case of DPS

illumination, a relatively small  $I_{diffusion}$  is generated due to the small amount of oxygen vacancies in the Ag/BLFO interfaces, and the  $I_{diffusion}$  might be smaller than  $I_{drift}$ , originating from the relatively large barrier height of Ag/BLFO compared with UPS. As a result, the DPS illumination induces only a negative photocurrent,  $I_{diffusion}$  flows to the upward direction (from LSMO to Ag in BLFO films).

With a similar scenario, we can understand the cases after downward or upward poling at 50K, which induces the polarization flipping, but also limits the electromigration of oxygen vacancies due to low ionic diffusion at low temperatures such as 50 K. For the upward poling at 50 K, the reduced  $I_{sc}$  may originate from the increase of  $I_{drift}$  due to the increase of the barrier height and from the decrease of  $I_{diffusion}$  because of the absence of oxygen vacancies near the Ag/BLFO interfaces, as shown in Fig. 4(c). For the downward poling at 50 K,  $I_{diffusion}$  becomes dominant and increases because of more oxygen vacancies near the Ag/BLFO interfaces, while  $I_{drift}$  reduces due to the reduction of barrier height, compared with Fig. 4(b). As a result,  $I_{sc}$  is positive when  $I_{diffusion}$  is bigger than  $I_{drift}$ , as shown in Fig. 4(d).

In the case of applying consistent negative pulse voltages on the BLFO films, more and more oxygen vacancies repelled and accumulated at, the Ag/BLFO interface, which induces a larger  $I_{diffusion}$  and smaller  $I_{drift}$  due to the relatively lower barrier of Ag/BLFO. Therefore, the variation of  $I_{sc}$  is positive both in UPS and DPS as shown in Figs. 4(e) and 4(f). As a result,  $I_{sc}$  can change it direction from upward to downward when  $I_{diffusion}$  is bigger than  $I_{drift}$ , consistent with the results in Fig. 3(b). Similarly, when applying consistent positive pulse voltages, as more and more oxygen vacancies repelled and accumulated at BLFO/LSMO interface, which induces  $I_{diffusion}$  decreased and  $I_{drift}$  increasing due to the relatively higher barrier of Ag/BLFO, the variation of  $I_{sc}$  is negative both in UPS and DPS as shown in Figs. 4(g) and 4(h). Therefore, all of our results can be qualitatively understood within the scenario of the variation of Ag/BLFO barrier where both polarization and oxygen vacancies are involved.

In summary, we have found that significant ferroelectric photovoltaic effects exist in BLFO. The direction of the photocurrent is reversely switchable accompanying polarization flipping by applying large external voltages. The rectification direction is always backward, independent of the ferroelectric polarization direction, whereas the photovoltaic current direction is opposite to that of polarization. The polarization clearly plays an essential role in the photovoltaic effects. On the other hand, we have shown that the electromigration of defects such as oxygen vacancies must be taken into account for the electric-field-induced switching. The photovoltaic effects as well as their switching behaviors can be explained with the concept of the variation of Ag/BLFO barrier resulting from the combination of polarization flipping and the electromigration of defects such as oxygen vacancies. We also found that the photovoltaic effect could be independent of the direction of polarization when the variation of the modulation of the Schottky barrier at the Ag/ $\text{Bi}_{0.9}\text{La}_{0.1}\text{FeO}_3$  interface induced by oxygen vacancies are large enough to offset those induced by polarization. By engineering the distribution of oxygen vacancies and polarization directions, these

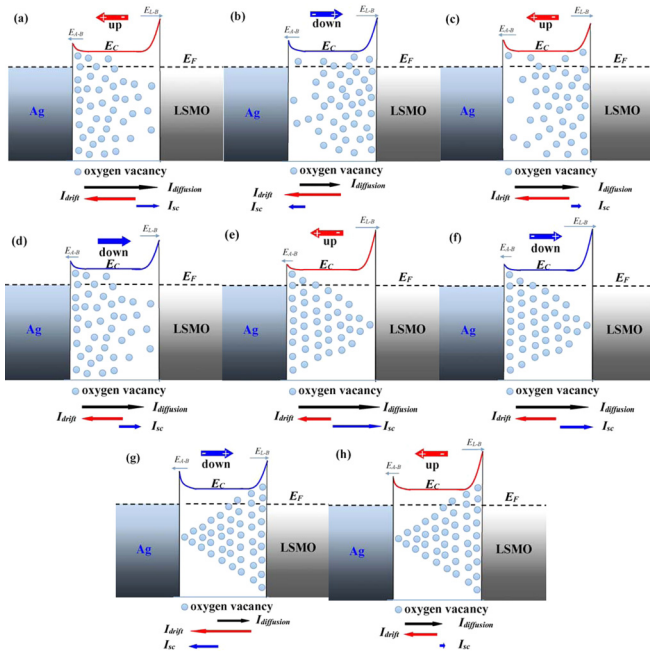


FIG. 4. Schematics energy band diagrams of Ag, BLFO, LSMO, and the variation of drift current ( $I_{drift}$ ), diffusion current ( $I_{diffusion}$ ) and the net photocurrent ( $I_{sc}$ ). (a) UPS, poled by  $-30$  V. (b) DPS, poled by  $+30$  V (c) UPS, poled by  $-30$  V at 50 K (d) DPS, poled by  $+30$  V at 50 K (e) UPS, poled by  $-30$  V pulse voltage strings for 1000 times. (f) DPS, poled by  $-30$  V pulse voltage strings for 1000 times and then poled with  $+30$  V. (g) DPS, poled by  $+30$  V pulse voltage strings for 1000 times. (h) UPS, poled by  $+30$  V pulse voltage strings for 1000 times and then poled with  $-30$  V.

fascinating switchable or nonswitchable effects can be exploited for novel technological devices such as ferroelectric sensors, fast readouts of ferroelectric state, or ferroelectric solar cells.

The present work has been supported by the National Basic Research of China, the National Natural Science Foundation of China, the Knowledge Innovation Project of the Chinese Academy of Sciences, and the Beijing Municipal Natural Science Foundation.

- <sup>1</sup>W. Prellier, M. P. Singh, and P. Murugavelet, *J. Phys.: Condens. Matter*, **17**, 7753 (2005).
- <sup>2</sup>W. Eerenstein, N. D. Mathur, and J. F. Scott, *Nature*, **442**, 759 (2006).
- <sup>3</sup>C. Michel, J.-M. Moreau, G. D. Achenbach, R. Gerson, and W. J. James, *Solid State Commun.* **7**, 701 (1969).
- <sup>4</sup>J. Wang, J. B. Neaton, H. Zheng, V. Nagarajan, S. B. Ogale, B. Liu, D. Viehland, V. Vaithyanathan, D. G. Schlom, U. V. Waghmare, N. A. Spaldin, K. M. Rabe, M. Wuttig, and R. Ramesh, *Science*, **299**, 1719 (2003).
- <sup>5</sup>T. Choi, S. Lee, Y. Choi, V. Kiryukhin, and S. Cheong, *Science*, **324**, 63 (2009).
- <sup>6</sup>W. Ji, K. Yao, and Y. Liang, *Adv. Mater.* **22**, 1763(2010).
- <sup>7</sup>H. T. Yi, T. Choi, S. G. Choi, Y. S. Oh, and S.-W. Cheong, *Adv. Mater.* **23**, 3403 (2011).
- <sup>8</sup>S. Y. Yang, J. Seidel, S. J. Byrnes, P. Shaferl, C.-H. Yang, M. D. Rossell, P. Yu, Y.-H. Chu, J. F. Scott, J. W. Ager III, L. W. Martin, and R. Ramesh, *Nature. Nanotechnol.* **5**, 143 (2010).
- <sup>9</sup>S. Y. Yang, L. W. Martin, S. J. Byrnes, T. E. Conry, S. R. Basu, D. Paran, L. Reichertz, J. Ihlefeld, C. Adamo, A. Melville, Y.-H. Chu, C.-H. Yang, J. L. Musfeldt, D. G. Schlom, J. W. Ager III, and R. Ramesh, *Appl. Phys. Lett.* **95**, 062909 (2009).
- <sup>10</sup>J. Seidel, D. Fu, S. Y. Yang, O. L. Alarc, J. Wu, R. Ramesh, and J. W. Ager III, *Phys. Rev. Lett.* **107**, 126805(2011).
- <sup>11</sup>R. Moubah, O. Rousseau, D. Colson, A. Artemenko, M. Maglione, and M. Viret, *Adv. Funct. Mater.* **22**, 4814(2012).
- <sup>12</sup>P. Zhang, D. Cao, C. Wang, M. Shen, X. Su, L. Fang, W. Dong, and F. Zheng, *Mater. Phys. Chem.* **135**, 304(2012).
- <sup>13</sup>B. Chen, Z. Zuo, Y. Liu, Q. F. Zhan, Y. Xie, H. Yang, G. Dai, Z. Li, G. Xu, and R. W. Li R, *Appl. Phys. Lett.* **100**, 173903(2012).
- <sup>14</sup>R. L. Gao, Y. S. Chen, J. R. Sun, Y. G. Zhao, J. B. Li, and B. G. Shen, *J. Appl. Phys.* **113**, 183510 (2013).
- <sup>15</sup>G. L. Yuan, L. W. Martin, R. Ramesh, and A. Uedono, *Appl. Phys. Lett.* **95**, 012904(2009).
- <sup>16</sup>R. L. Gao, Y. S. Chen, J. R. Sun, Y. G. Zhao, J. B. Li, and B. G. Shen, *Appl. Phys. Lett.* **101**, 152901(2012).
- <sup>17</sup>J. Dho, X. D. Qi, H. Kim, J. L. MacManus-Driscoll, and M. G. Blamire, *Adv. Mater.* **18**, 1445 (2006).
- <sup>18</sup>H. Béa, M. Bibes, S. Fusil, K. Bouzehouane, E. Jacquet, K. Rode, P. Bencok, and A. Barthélémy, *Phys. Rev. B*, **74**, 020101R (2006).
- <sup>19</sup>Y. H. Chu, Q. Zhan, L. W. Martin, M. P. Cruz, P. L. Yang, G. W. Pabst, F. Zavaliche, S. Y. Yang, J. X. Zhang, L. Q. Chen, D. G. Schlom, I. N. Lin, T. B. Wu, and R. Ramesh, *Adv. Mater.* **18**, 2307 (2006).
- <sup>20</sup>H. W. Jang, D. Ortiz, S. H. Baek, C. M. Folkman, R. R. Das, P. Shafer, Y. Chen, C. T. Nelson, X. Q. Pan, R. Ramesh, and C. B. Eom, *Adv. Mater.* **21**, 817 (2009).
- <sup>21</sup>S. V. Kalinin, D. A. Bonnell, T. Alvarez, X. Lei, Z. Hu, and J. H. Ferris, *Nano Lett.* **2**, 589 (2002).
- <sup>22</sup>J. L. Giocondi and G. S. Rohrer, *Chem. Mater.* **13**, 241 (2001).
- <sup>23</sup>S. Habicht, R. J. Nemanich, and A. Gruverman, *Nanotechnology* **19**, 495303 (2008).
- <sup>24</sup>C. H. Yang, J. Seidel, S. Y. Kim, P. B. Rossen, P. Yu, M. Gajek, Y. H. Chu, L. W. Martin, M. B. Holcomb, Q. He, P. Maksymovych, N. Balke, S. V. Kalinin, A. P. Baddorf, S. R. Basu, M. L. Scullin, and R. Ramesh, *Nature Mater.* **8**, 485 (2009).
- <sup>25</sup>S. J. Clark and J. Robertson, *Appl. Phys. Lett.* **90**, 132903 (2007).
- <sup>26</sup>L. Pintilie and M. Alexe, *J. Appl. Phys.* **98**, 124103 (2005).
- <sup>27</sup>L. Hu, Z. G. Sheng, Y. N. Huang, W. H. Song, and Y. P. Sun, *Appl. Phys. Lett.* **101**, 042413 (2012).
- <sup>28</sup>R. Cauro, A. Gilbert, J. P. Contour, R. Lyonnet, M.-G. Medici, J.-C. Grenet, C. Leighton, and I. K. Schuller, *Phys. Rev. B* **63**, 174423 (2001).
- <sup>29</sup>Z. G. Sheng, Y. P. Sun, J. M. Dai, X. B. Zhu, and W. H. Song, *Appl. Phys. Lett.* **89**, 082503 (2006).